

# Consolidation Assessment of Marine Clay Using Electrokinetic Coupled with Constant Load

Deep Jyoti Singh, Bala Ramudu Paramkusam\*, Arun Prasad

Department of Civil Engineering, Indian Institute of Technology (BHU), Varanasi, Uttar Pradesh, India

Received July 25, 2022; Revised August 30, 2022; Accepted October 11, 2022

## Cite This Paper in the Following Citation Styles

(a): [1] Deep Jyoti Singh, Bala Ramudu Paramkusam, Arun Prasad, "Consolidation Assessment of Marine Clay Using Electrokinetic Coupled with Constant Load," *Civil Engineering and Architecture*, Vol. 10, No. 7, pp. 2886 - 2900, 2022. DOI: 10.13189/cea.2022.100709.

(b): Deep Jyoti Singh, Bala Ramudu Paramkusam, Arun Prasad (2022). Consolidation Assessment of Marine Clay Using Electrokinetic Coupled with Constant Load. *Civil Engineering and Architecture*, 10(7), 2886 - 2900. DOI: 10.13189/cea.2022.100709.

Copyright©2022 by authors, all rights reserved. Authors agree that this article remains permanently open access under the terms of the Creative Commons Attribution License 4.0 International License

**Abstract** In Marine clays, the consolidation phenomenon is a significant issue of concern. For this, an innovative electrokinetic consolidation method was adopted by coupling the conventional consolidation technique with a constant voltage gradient. A series of tests were performed on reconstituted marine clay samples for constant loading intensity of 4kg/cm<sup>2</sup> coupled with a constant DC voltage of 2, 4 and 6V. Various parameters such as deformation, void ratio, current, pH, voltage and moisture content were continuously monitored to compare with test results of conventional Incremental loading (IL) and constant loading (CL) techniques. In the case of electrokinetic (EK) coupled loading, with an increase in voltage gradient, the values obtained for voltage and current were also increased to maximum and then decreased afterwards. Microfabric changes were also visible in soils collected at anode and cathode, which were evidenced with the images of scanning electron microscopy (SEM) data obtained before and after EK consolidation tests when compared with original marine clay. The constant loading intensity of 4kg/cm<sup>2</sup> with a 4V electric gradient resulted in higher compression and better consolidation characteristics than other loading conditions.

**Keywords** Marine Clay, IL Consolidation, EK Consolidation, Voltage Gradient, Compression

electro-osmosis treatment for rapid movement of water from anode front to cathode front on the application of direct current (DC) in a saturated porous medium [1,2]. Later, Casagrande explored electrokinetic (EK) technology to reinforce soft/problematic soils and slopes in 1952 [3]. Many other researchers also contributed to the advancement of EK technology in geotechnical and geoenvironmental applications. The problems associated are excessive deformation in foundations, decrease of swelling and shrinkage in capacity, increase in friction pile capacity, stabilization and strengthening of soft clays, consolidation of marine and dredged sediments for land reclamations and dewatering of slurries, sludges and mine tailings [4–11]. In the current era of technology, Electro-osmotic (EO) consolidation is a potential technique for accelerated pore pressure dissipation and resulting in the early consolidation of soft soils and dredged sediments with high moisture content, low compressibility, low permeability and low bearing capacity. Based on prior research, electro-osmotic consolidation proved to be an economical and time-saving method for treating low permeable soft soils [7, 12–14]. Critical laboratory-scale studies should be performed for field application to predict the feasibility, suitability, availability of resources, cost-effectiveness and time consumption of the process and to anticipate the influence of potential gradient and its effect on the required parameters [4, 15–17].

Conventional laboratory apparatus with 2cm in height and 6cm in diameter is suitable for routine Incremental Loading (IL) as mentioned in [18]. Numerous researchers

## 1. Introduction

In 1809, Reuss discovered the fundamental principles of

carried out a study on their modified versions of consolidation tests with varying sizes, shapes, loading intensities, load increment ratios and materials to measure and estimate the relevant parameter for field conditions. However, in the case of electro-osmosis consolidation, no such standard code of practice is available. To carry out the test, EK coupled loading consolidation setup is designed and fabricated as per the standard protocols mentioned in ASTM D2435M-11 with a D/H ratio equivalent to 2.5 and considering the surface friction of the consolidometer. Some of the essential considerations for the setup required for the electro-osmosis test are:

1. Easy provision for the expulsion of developed gases
2. Continuous automated data monitoring with Data Acquisition System (DAQ) at regular time intervals without interruption
3. Availability and suitability of sensor with DAQ for multiple parameter deformation/settlement, current and voltage measurement with time

The present paper discusses a detailed design and experimental outline of EK coupled constant loading consolidation (EKCL) setup and procedure involved with the reconstituted marine soil sample preparation and later compared with the data obtained from conventional IL and CL consolidation tests. A series of tests were conducted under different loading conditions of IL consolidation upto  $4 \text{ kg/cm}^2$  and CL consolidation with  $4 \text{ kg/cm}^2$  single load on a modified consolidation ring. Further EKCL

consolidation tests were performed with constant loading of  $4 \text{ kg/cm}^2$  coupled with constant DC Voltage application of 2, 4 and 6V without any lateral deformation was performed using a modified consolidation ring. During the test, the Data Acquisition system continuously monitored settlement, voltage and current. After completion of the test, the void ratio, bulk and dry density, water content and pH values were also measured. The main objective is to validate the test results of EK coupled consolidation with reference to conventional IL tests; thus, a system and method for faster determination of the compressibility and consolidation characteristics of fine-grained soils will be recommended.

## 2. Materials and Methods

### 2.1. Materials

In the present study, a disturbed marine soil sample was collected from the depth of 0.5m from the reclamation area at Jawahar Nehru Port Trust (JNPT), Mumbai, Maharashtra, India. The sample obtained was grey-black coloured; it was then air and oven-dried, pulverized with the mallet and then sieved using a 4.75mm sieve to remove any unwanted foreign particles. The physical and geotechnical properties of soil are evaluated as per relevant ASTM codes as presented in **Table 1**.

**Table 1.** Physical and geotechnical properties of marine soil

| Properties                                    | Standard code/Procedure used | Values        |
|---|------------------------------|---------------|
| Specific gravity                              | [19]                         | 2.6           |
| Clay (%)                                      | [20]                         | 66.0          |
| Silt (%)                                      |                              | 23.0          |
| Sand (%)                                      |                              | 11.0          |
| Classification (USCS)                         |                              | CH            |
| Natural water content (%)                     | [21]                         | 108.0         |
| Liquid limit (%)                              | [22]                         | 82.0          |
| Plastic limit (%)                             |                              | 46.0          |
| Optimum moisture Content (OMC) (%)            | [23]                         | 33.0          |
| Maximum dry density (MDD) ( $\text{Mg/m}^3$ ) |                              | 1.39          |
| pH  | [24]                         | 8.1           |
| Organic content (%)                           | [25]                         | 6.34          |
| Colour  | -                            | Greyish black |

## 2.2. Electrodes

The past investigation showed that copper electrodes were the best suitable and the same was used in the present study. The main advantages of the utilization of copper electrodes are its high electrical conductivity, good electrical conductance, reduced power loss at the electrode front, easy availability and reasonable cost [4, 26, 27]. The electrode diameter, thickness and total area were 9.4cm, 0.2cm and 69.36cm<sup>2</sup>, respectively. Multiple holes of 1 mm diameter were made to facilitate the pore water dissipation, and a layer of saturated filter paper was placed over the electrode at the top and bottom to avoid clogging the holes. During the experiment, an electrolysis reaction occurred, and oxygen gas was generated at the anode front, where copper is utilized at the cathode front to form copper oxide. The metal reactions involved with oxidation and reduction reactions are mentioned below:

Oxidation at the anode:



Reduction at the cathode:



which represent copper electrode in an oxidation reaction and result in the formation of the copper ion with valence 2 in solution and represent the copper precipitate in solution.

## 2.3. Sample Preparation and Experimental Setup

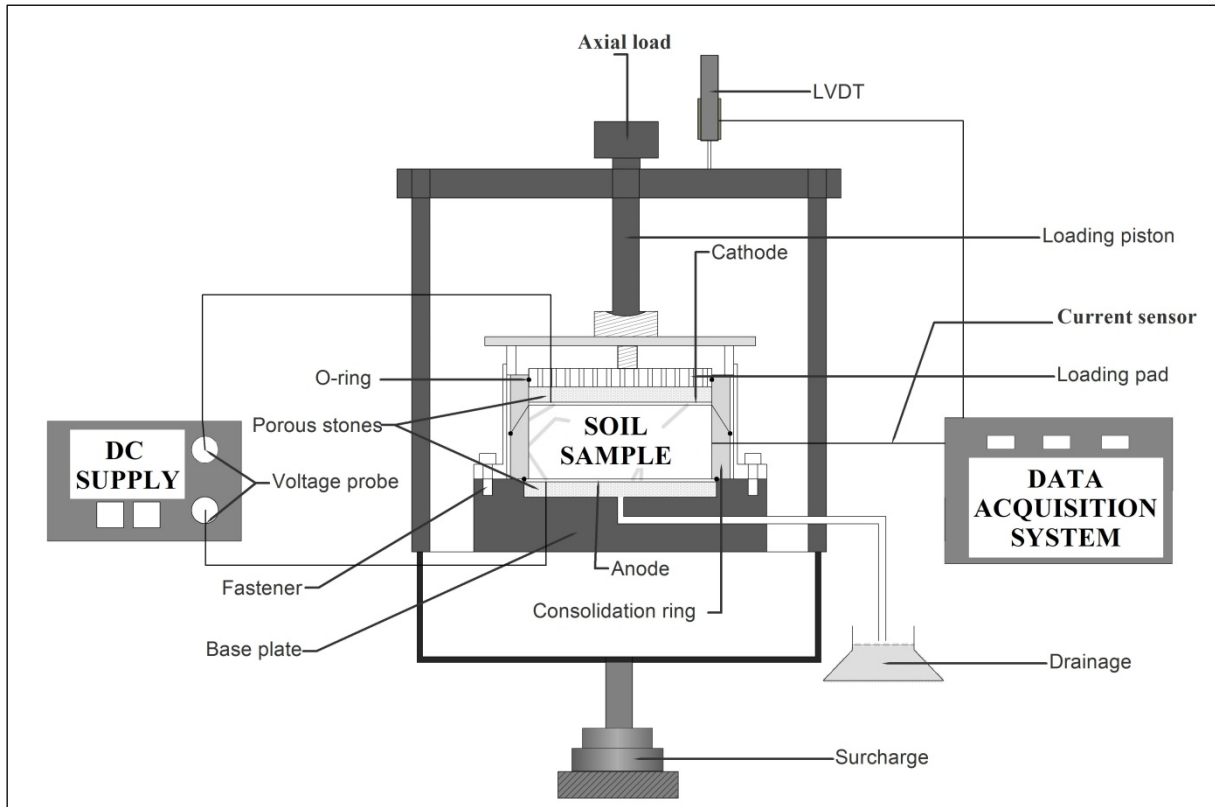
For the experiment, reconstituted marine soil samples were prepared using the slurry consolidation technique to ensure a fully saturated consolidated sample [28].

To meet the current study's research requirements, EK coupled constant loaded consolidation experimental setup was indigenously designed and fabricated for conducting the laboratory electro-osmotic consolidation tests. The main embodiment of EKCL setup comprises a consolidation ring of size 100mm in diameter and 40mm in

height and was made of Teflon coated stiff steel material to provide better surface insulation, corrosion resistance, and sample housing. The base plate has a provision to support the consolidation ring and mechanical load application facility regarding the consolidation ring size. Two copper electrode discs, acting as anode and cathode at the top and bottom of the consolidation ring, were provided to enhance the pore water dissipation faster on applying a constant voltage. Two porous stones and filter paper were arranged on the bottom and top of the sample to prevent the entry of the soil particles from the consolidation ring and to allow free water flow. A perforated loading pad was placed over the top porous stone of consolidation ring assembly. A linear variable displacement transducer (LVDT) is placed over loading pad to measure the axial settlement continuously with different loading conditions. Current sensor and Voltage sensor were used to measure current and voltage throughout the sample during the test. A collar ring was placed to support the consolidation ring at the predefined position with the base plate with multiple fasteners. Finally, a Data Acquisition System (DAQ) was connected to the sensors to measure and store the data at regular intervals throughout the process. A DC supply source was included to provide the DC supply and maintain an electric gradient throughout the experiment. A schematic diagram of the experimental setup with various components of the present EKIL consolidation is shown in Figure 1.

## 2.4. Experimental Procedure

The experimental plan includes a series of experiments performed with defined loading intensity and over the range of voltage gradient. Five different loading conditions were followed in the study, amongst which three were coupled constant loading of 4kg/cm<sup>2</sup> coupled with DC voltage of 2, 4 and 6V and two tests were carried out by placing of 4kg/cm<sup>2</sup> either direct or as in the form of incremental loading intensity without DC voltage.



(a)



(b)

**Figure 1.** (a) One Dimensional Electro-Osmotic Consolidometer; (b) Experimental setup

To initiate the experiment, a reconstituted marine soil sample was extracted and weighed from the slurry consolidation technique, including the consolidation ring before and after the tests performed to evaluate the soil moisture content pre and post-experiment conditions. Then copper electrode discs were positioned at the top and bottom of the soil to act as cathode and anode connected to an active DC supply for a constant Voltage application. Next, porous stones and filter paper were placed after the electrodes were positioned. The loading pad was placed at the top of the consolidation ring for the distribution of the applied constant load. Afterwards, the collar was placed, connecting the consolidation ring and the base plate with fasteners. This base plate consists of two openings, the first for electrical wiring and the second for discharge of the gas and fluid generated during the test.

Voltage and current sensors were attached to a metal probe at the mid-level of the sample from one end and DAQ at another. After assembling the whole consolidation ring setup, a surcharge load of  $0.05\text{kg/cm}^2$  was placed over the sample through a lever arrangement with a load distribution ratio equal to 1:10 on the loading assembly. At the time of commencement of the experiment, the DC supply and DAQ were turned on and checked for zero adjustment reading of LVDT, voltage and current reading for EKCL loading at a constant voltage (equal to 2, 4 and

6V) application and simultaneously a constant load of  $4\text{kg/cm}^2$  was placed on the sample. The DAQ provides an automated collection and storage of various data during the process at a fixed interval with an RS-232 interface.

The analysis of results showed that the voltage becomes stable to an extent whereas current trend kept decreasing with the progress of the test due to increased resistance with time and the dissipation of pore water. During the test, the gas generated throughout the electrolysis process is visible at the top and bottom in the form of bubbles. In the case of mechanical loading, two types of loading conditions: constant loading of  $4\text{kg/cm}^2$ , and incremental loading up to  $4\text{kg/cm}^2$  on the modified consolidation setup without voltage and readings are taken at fixed intervals to calculate the settlement.

### 3. Results and Discussions

The current setup facilitates mechanical and coupled electro-mechanical loading for faster pore water pressure dissipation in the vertical direction for one-dimensional consolidation. The results obtained from the various tests are mentioned in Table 2. The test on Marine soil was carried out at five different mechanical loading conditions with and without constant electric gradient.

**Table 2.** Test results from EKIL and conventional techniques

| Loading   | Modified Consolidometer                  |                       |                       |  |                                  | Conventional Consolidometer                 |
|---|--|-----------------------|-----------------------|--|----------------------------------|---|
|   | DC Voltage Coupled with Constant Loading |                       |                       | Without DC Voltage                         |                                  | Incremental loading up to $4\text{kg/cm}^2$ |
|   | 2V+ $4\text{kg/cm}^2$                    | 4V+ $4\text{kg/cm}^2$ | 6V+ $4\text{kg/cm}^2$ | Incremental loading upto $4\text{kg/cm}^2$ | Direct loading $4\text{kg/cm}^2$ |   |
| Max. settlement at the end of loading (mm)                  | 12.121                                   | 12.36*                | 12.298                | 9.923                                      | 9.286                            | 5.3   |
| Final settlement at the end of unloading (mm)               | 11.376                                   | 11.873*               | 11.64                 | 8.53                                       | 7.844                            | 4.82  |
| Time to reach final settlement (hrs)                        | 52.5                                     | 84.9                  | 31.933*               | 144.6                                      | 114.27                           | 144.6                                       |
| Settlement for average degree of consolidation ( $U_{50}$ ) | 6.11                                     | 6.216                 | 6.211                 | 4.964                                      | 4.698                            | ---   |
| Time to reach average degree of consolidation ( $U_{50}$ )  | 0.534                                    | 0.817                 | 0.567                 | 75.334                                     | 0.379                            | ---   |
| Settlement for average degree of consolidation ( $U_{90}$ ) | 10.914                                   | 11.126                | 11.079                | 8.948                                      | 8.366                            | ---   |
| Time to reach average degree of consolidation ( $U_{90}$ )  | 4.55                                     | 6.98                  | 3.56                  | 120.5                                      | 2.652                            | ---   |
| Percentage regain (%)                                       | 6.55                                     | 4.102*                | 5.653                 | 16.33                                      | 18.38                            | 9.95  |
| Initial void ratio  | 1.649                                    | 1.626*                | 1.648                 | 1.624                                      | 1.631                            | 1.638                                       |
| Final void ratio  | 0.846                                    | 0.8279*               | 0.834                 | 0.983                                      | 1.02                             | 0.939                                       |
| Water content (%)   | 62.688                                   | 62.646*               | 62.102                | 61.9                                       | 61.65                            | 61.68                                       |

Table 2 Continued

|  |                       |                       |                       |                       |                       |                       |
|--|-----------------------|-----------------------|-----------------------|-----------------------|-----------------------|-----------------------|
| Density before test (kN/m <sup>3</sup> )                   | 16.24                 | 16.33 <sup>*</sup>    | 16.42                 | 16.242                | 16.324                | 16.28                 |
| Density after test (kN/m <sup>3</sup> )                    | 9.98                  | 10.04 <sup>*</sup>    | 10.13                 | 10.03                 | 10.09                 | 10.07                 |
| Coefficient of volume change (per kPa)                     | $7.57 \times 10^{-4}$ | $7.73 \times 10^{-4}$ | $7.69 \times 10^{-4}$ | $5.32 \times 10^{-4}$ | $5.8 \times 10^{-4}$  | $4.94 \times 10^{-4}$ |
| Coefficient of compressibility- $a_v$                      | $2.01 \times 10^{-3}$ | $2.02 \times 10^{-3}$ | $2.04 \times 10^{-3}$ | $2.83 \times 10^{-3}$ | $1.53 \times 10^{-3}$ | $1.31 \times 10^{-3}$ |
| Coefficient of consolidation- $c_v$ (mm <sup>2</sup> /sec) | $2.81 \times 10^{-2}$ | $1.99 \times 10^{-2}$ | $3.13 \times 10^{-2}$ | $1.87 \times 10^{-2}$ | $8.35 \times 10^{-2}$ | $6.46 \times 10^{-2}$ |
| At anode   | 34.216                | 33.865                | 33.744                | -                     | -                     | -                     |
| At cathode   | 40.320                | 37.792                | 38.883                | -                     | -                     | -                     |
| Initial Water content                                      | 62.688                | 62.646                | 62.102                | 61.9                  | 61.65                 | -                     |

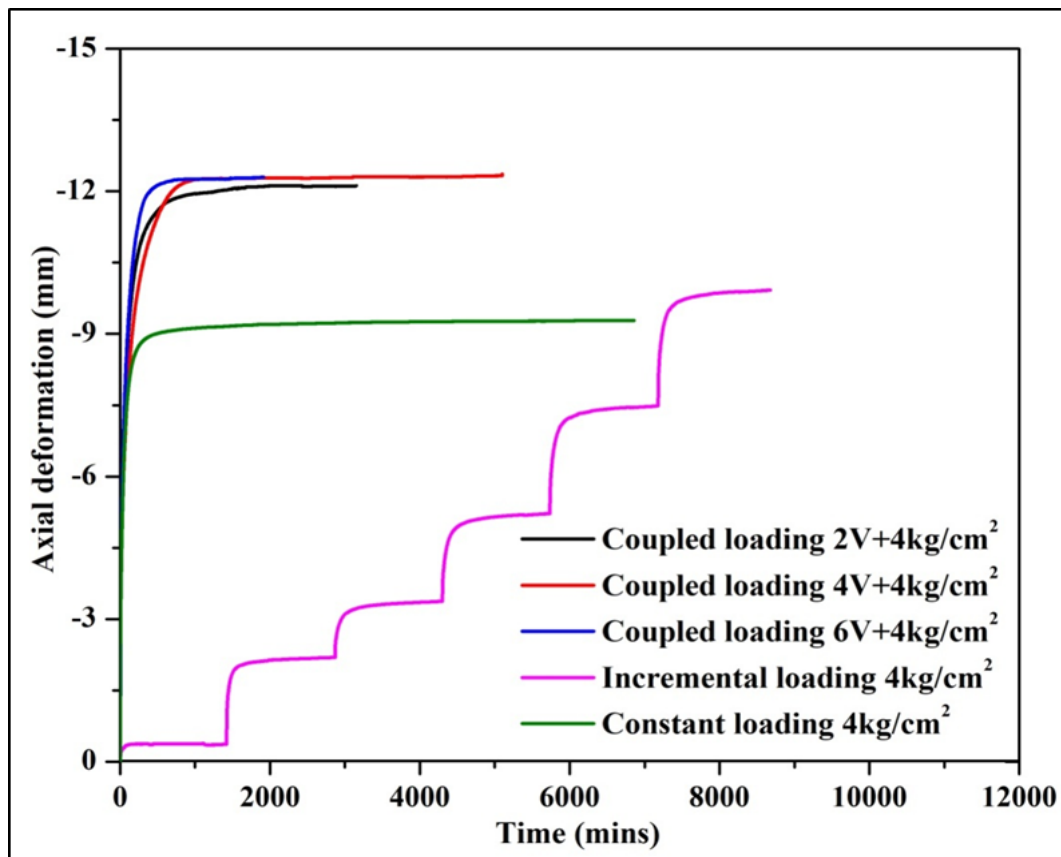


Figure 2. Axial deformation with time for different loading conditions

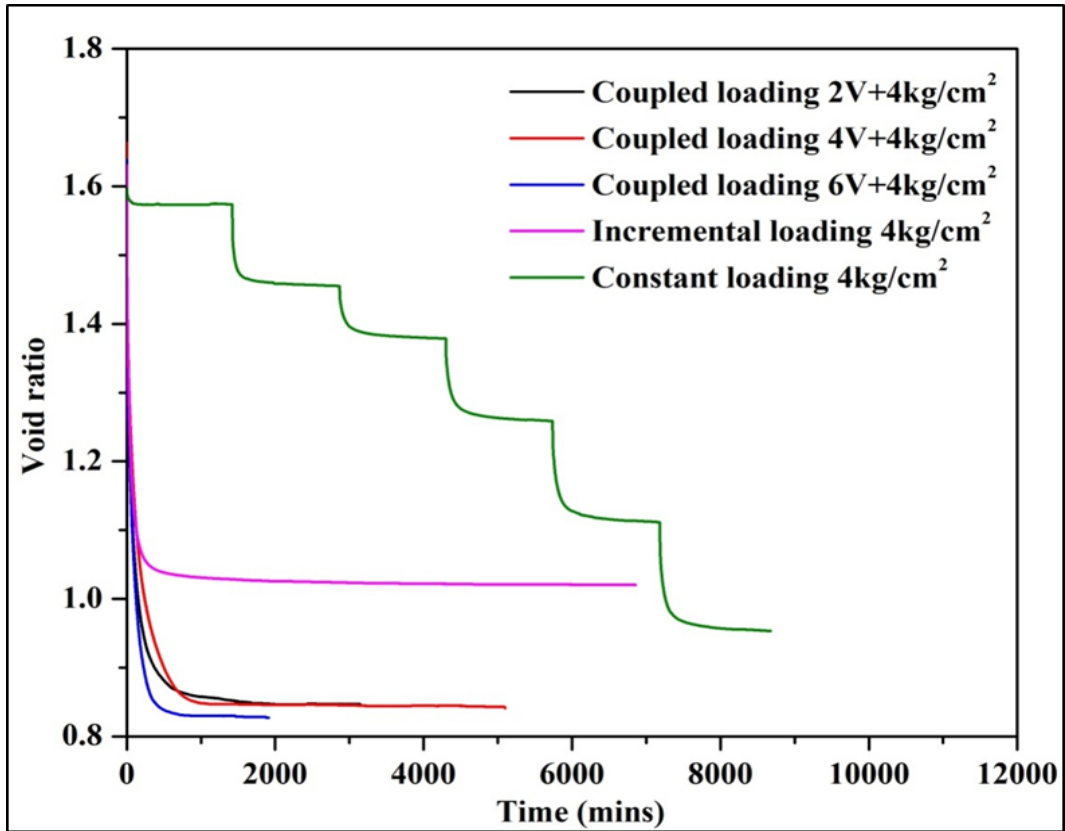


Figure 3. Void ratio with time for different loading conditions

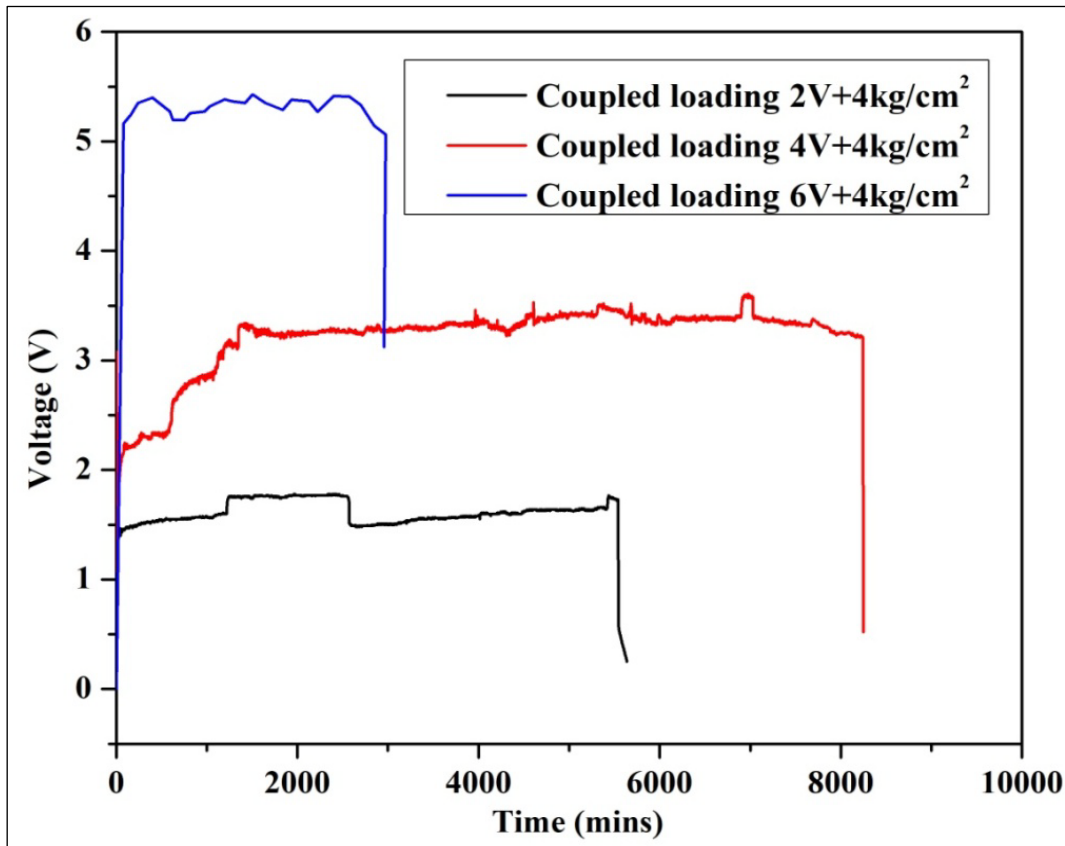


Figure 4. Voltage with time for coupled electro-mechanical loading conditions

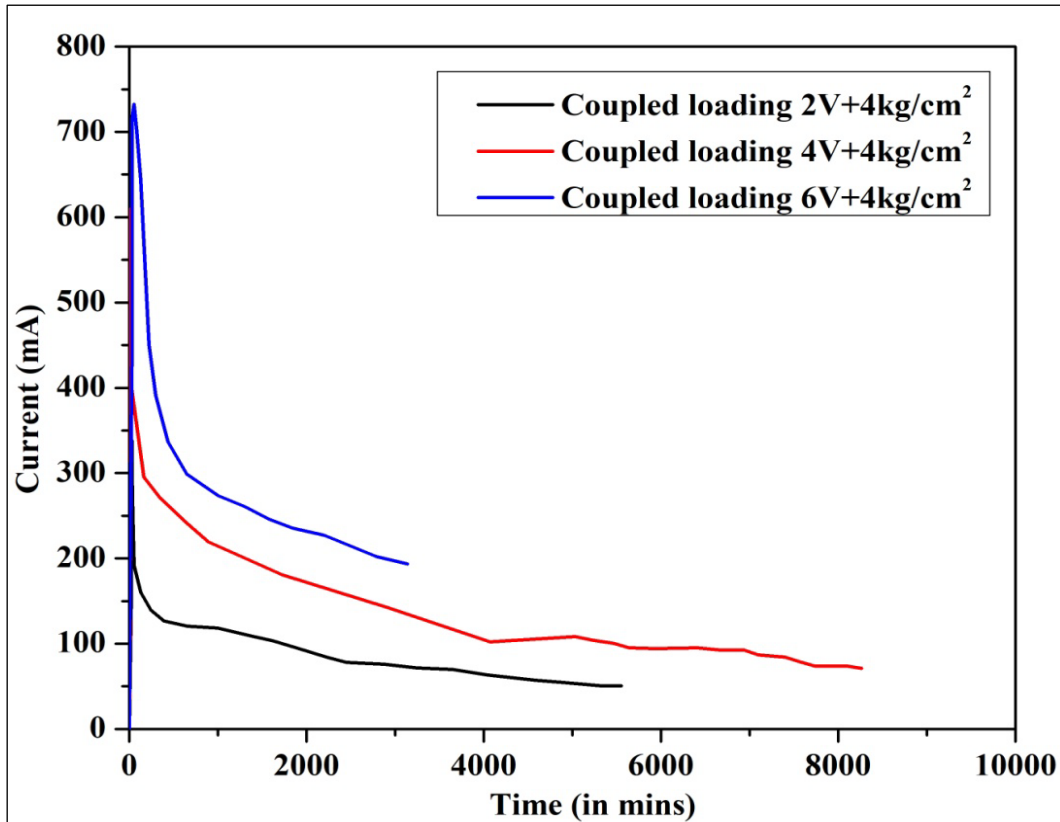


Figure 5. Current with time for coupled electro-mechanical loading conditions

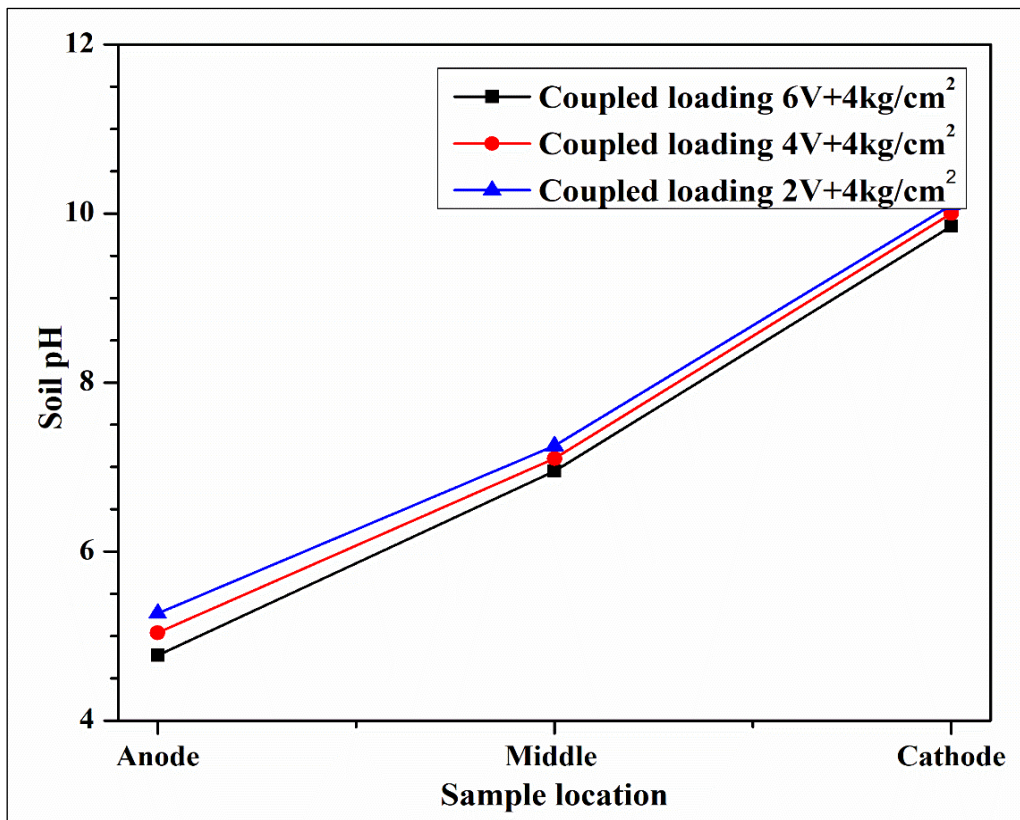


Figure 6. pH vs sample location for coupled electro-mechanical loading conditions

### 3.1. Axial deformation vs. Time

Figure 2 illustrates the characteristic trend of soil deformation with time for different loading conditions (Table 2) observed in the case of a modified oedometer. A Linear Variable Differential Transducer (LVDT) is placed on the top of the loading pad to measure the continuous deformation of the soil sample. An increased settlement with time was observed in electro-hydro-mechanical coupled loading compared to mechanical loading [29].

This additional settlement is due to the electro-osmotic flow process, which includes the transport of ions under an electric gradient. The ion transport in the phenomenon includes diffusion, electromigration and electro-osmotic flux advection [30]. Thus it results in faster dissipation of excess pore water that alters the soil fabric due to pore fluid flow, ion migration, and charged particle flow [31,32]. The electro-osmotic flow was directly proportional to the applied electric potential. It was observed that a maximum settlement of 12.36 mm occurs in the case of coupled loading of 4V+4kg/cm<sup>2</sup> in comparison to other loading conditions. Based on the past studies, the maximum compression occurs for a voltage gradient of 1V/cm, same trend was also observed in the case of 4V+4kg/cm<sup>2</sup> in the present study, equivalent to a voltage gradient of 1V/cm [33–36].

### 3.2. Void Ratio vs. Time

Figure 3 illustrates the variation of the void ratio with time for different loading conditions. It is well known that the void ratio is inversely proportional to effective stress and directly proportional to pore water pressure. With the development of negative excess pore pressure, the effective stress in the soil increases, resulting in a decreased void ratio with time. A maximum reduction in the void ratio was observed in EK coupled loading as mentioned in Table 2. Based on the theory, the decrease in the void ratio is basically due to an additional increase in the expulsion of pore water in case of coupled loading consolidation. The void ratio and volume change behavior are similar to those of trends expected in the consolidation process adopted through mechanical loading. Based on past studies, the maximum reduction in void ratio and volume change occurred for voltage gradient equals unity which can also be validated with the test results obtained in the current study.

### 3.3. Voltage vs. Time

Voltage is an additional parameter obtained for three different electrokinetic coupled mechanical loading cases in which electric gradient plays an important role throughout the test (Figure 4). In the study, continuous monitoring of Voltage data was performed at the mid-height of the soil sample and recorded through the

voltage sensor attached to the DAQ. The graph shows the consistent result with past findings and a significant voltage loss for constant voltage application on soil specimens. Many researchers also reported similar findings [29, 37, 38]. The Voltage loss that occurred in the vicinity of the anode was found to be less than at the cathode [39]. This voltage loss results from the precipitation of metal hydroxides near the cathode and the desorption of metal ions at the anode. The efficiency factor was increased with an increase in applied voltage; the same was observed by other researchers also [29,30]. The results indicate that an increase in voltage gradient improves the effective voltage with reference to the output voltage during the early stage of the electro-osmotic process. However, from a long-term perspective, an increase of the voltage gradient alone is not helpful in increasing the effective voltage to the output voltage.

### 3.4. Current vs. Time

Current is also an additional parameter monitored throughout the test for different electrokinetic coupled mechanical loadings and Figure 5 depicts a variation in current with time. It is observed that the current drops rapidly in the initial phase and reaches a stable value of 42, 57 and 175mA at 2V+4kg/cm<sup>2</sup>, 4V+4kg/cm<sup>2</sup> and 6V+4kg/cm<sup>2</sup> respectively in case EK coupled loadings. A similar variation of current was reported by several researchers [4, 37, 40]. The drop-off in current with time is due to the electrochemical changes leading to an increased rate in the formation of the gas bubble with time. It increases the resistance between the anode and cathode, resulting in the reduction of ion mobility, current intensity and consolidation efficiency [40, 41]. Initially, as the voltage gradient is applied acidic and basic front was generated at anode and cathode which causes heterogeneous ion concentration in the soil-water system. This heterogeneous ion concentration reduces the electrical conductivity of soils and releases the H<sup>+</sup> ions in the expelled pore fluid near the anode [29, 42].

### 3.5. pH vs. Sample location

pH is also an additional parameter that needs to be considered during the electrochemical process, and OH<sup>-</sup> ion is transferred from cathode surface to anode [43]. This leads to the H<sup>+</sup> ion movement from the anode surface to the cathode to neutralize and obstruct OH<sup>-</sup> ion movement [8, 44]. In clay particles, the H<sup>+</sup> is adsorbed by negatively charged clay particles due to its buffering capacity this results in increased pH value from the anode (bottom) to cathode (top) as shown in Figure 6. In addition, with an increase in voltage, the movement of H<sup>+</sup> and OH<sup>-</sup> ions will increase which results in a higher variation of pH value. Similar observations were also reported by other researchers [9, 29, 44, 45]



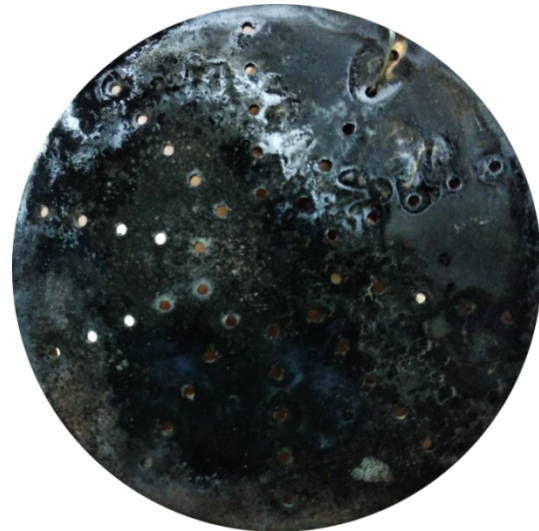
(a.) Bubble formation during the initial stage of coupled loading



(b.) Top view of consolidation ring after completion of the test



(c.) The copper electrode at the Anode front after the test



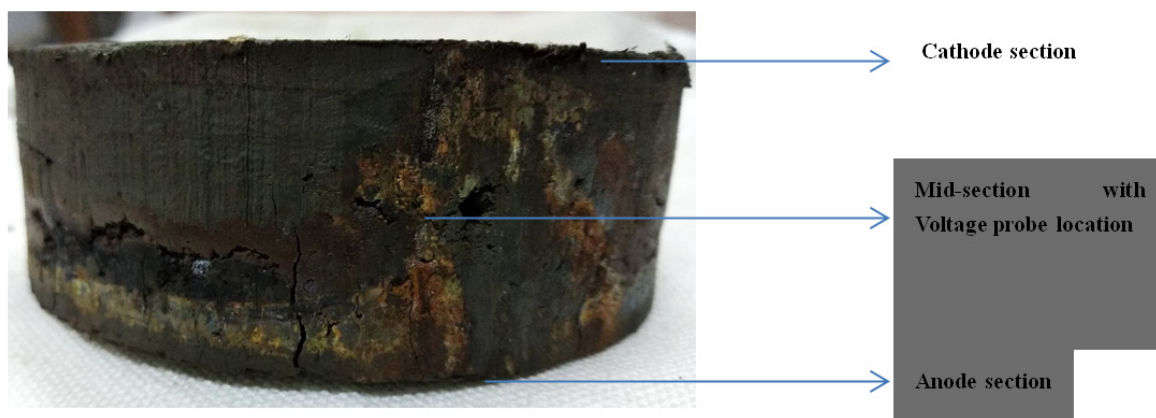
(d.) The copper electrode at Cathode front after test



(e.) Soil sample at anode front



(f.) Soil sample at cathode front



(g.) Soil sample after test

**Figure 7.** Images soil and electrodes before and after the coupled loading test

### 3.6. Moisture Content of Soil

The moisture content of the soil samples for pre and post EK consolidation, tests subjected to different mechanical and coupled electro-mechanical loading conditions were found and reported in Table 2. In the case of EK consolidation, the fluid movement resulting from the electrochemical changes and complex mechanism leads to non-uniform moisture content across soil samples was observed [39]. The reason behind the phenomenon is the movement of positively charged particles towards the cathode (negative front), while negatively charged particles toward the anode (positive front). This is due to the accelerated expulsion of interstitial water under applied electric gradient which ultimately consolidates the soil. On the other end, a uniform distribution of moisture content was observed only in mechanical loading.

### 3.7. Images before and after Consolidation Test

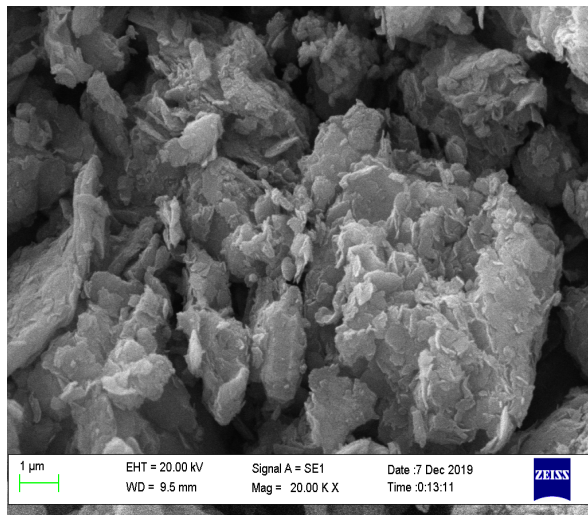
Coupled electromechanical loading tests performed on reconstituted marine soil sample have resulted in the expulsion of additional pore-water that leads to an increased volume reduction. The interpretation of data obtained from coupled electro-mechanical loading tests such as deformation, void ratio and water content after the test validates the success of the EK consolidation technique when compared to conventional IL test. Few photographs related to the coupled experiment are shown in Figure 7 for a better understanding of the chemical and physical changes taking place in soil and electrodes after the electrochemical action.

Figure 7(a) depicts the formation of a gas bubble during the initial stages of the consolidation test run with EK coupled constant loading. However, gas formation is taking place due to the electrolysis of soil and was

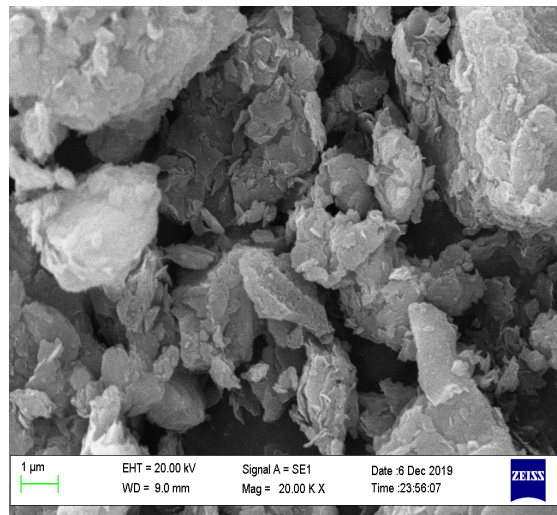
observed to be directly proportional to the voltage applied. Figure 7(b) shows the final stage of EK coupled loading. At the end of the test, heavy deposition of electrode precipitation was observed on the loading pad and precipitation occurred as a result of the electrokinetic phenomenon at the cathode front which increased the resistivity of soil. Figure 7(c) shows the deteriorated condition of the copper electrode (Anode) after completion of the test due to the complex phenomenon involved with the electrokinetic coupled test and oxidation of copper electrode and generation of oxygen gas. Figure 7(d) shows the deteriorated condition of the copper electrode (cathode) after the completion of the test due to the complex phenomenon involved with the electrokinetic coupled test and reduction of the copper electrode and generated hydrogen gas. A higher loss of moisture content in soil at the anode in comparison to the cathode was observed and the anode and cathode sides of the soil are shown in Figure 7 (e) and (f) respectively. Figure 7 (g) shows the side view of the sample after removing it from the consolidation ring.

### 3.8. Scanning Electron Microscopy (SEM)

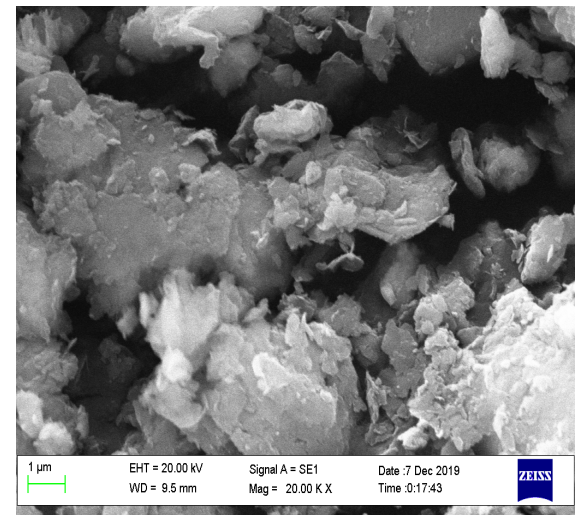
The microfabric/particle arrangement of soil can be investigated with representative scanning electron microscopy (SEM) of the dried soil before and after the electro-osmosis process [40]. Soil properties and characteristics depend on the intermediate microstructure of dispersed and flocculated soil [43,46–48]. The compressibility and consolidation characteristics are the results of clay matrices, interstitial pore spaces, diffuse double layer (DDL), and soil particles aggregation [42,49] These physical characteristics can be recognized with the SEM image for all microstructure features like particle arrangements, particle assemblage and pore spaces [50]



**At anode front**



**Original soil**



**At cathode front**

**Figure 8.** SEM images of marine soil at anode, original and cathode section

Figure 8 shows the induced microfabric changes within the inter-electrode space for coupled loading ( $4V+4kg/cm^2$ ) when compared with the original soil sample. An alteration in micro-fabric can be seen in the image. The microfabric size increased due to the contraction of the DDL envelope and bonding with the negatively charged particle. Another main characteristic is the redistribution of pore size visible within the treated soils. At the anode front, the size of micro aggregates decreased sharply in a highly acidic medium due to the dissolution of clay particles but at the cathode front, micro-aggregates size increased. Electro-osmosis caused the formation of anisotropic large pores (macropores) within the cathode and anode zone. Similar findings were also reported by Korolev and Nesterov (2019).

#### 4. Conclusions

A series mechanical and electro-hydro-mechanical experiments were performed to explore the mechanism for one-dimensional consolidation on a modified consolidation ring (100mm dia and 40mm height) in an axial direction with incremental loading up to  $4 kg/cm^2$  and constant loading  $4 kg/cm^2$  with and without voltage gradient of 2, 4 and 6V application. The parameter studied from the test data is deformation, voltage, current, pH, void ratio and moisture content. Based on these parameters, experimental data is compared, analysed and further validated. Based on these experimental investigations following conclusions can be made.

1. The present setup investigates coupled electro-hydro-mechanical loading effect on consolidation using indigenously designed laboratory setup with the provision of the expulsion of gases generated due to complex electro-hydro-mechanical phenomenon at the anode and cathode end.
2. Electro-hydro-mechanical coupled phenomenon is more advantageous than mechanical due to additional stresses generated in presence of electric gradient and resulted in an increased amount of effective settlement which consequently decreases the void ratio and changes the permeability of the soil. The maximum settlement was observed for a 1V/cm voltage gradient. This proves to be a notable impact in EK coupled loading due to the transport of ions includes diffusion, electromigration and electro-osmotic flux advection.
3. In electro-hydro-mechanical coupled consolidation, a sufficient voltage loss was observed at midheight of sample due to soil-electrode contact resulting in power loss. This voltage loss is attributed to electrode corrosion, gas generation and heating. The effective voltage at mid of sample was around 70-80% of the applied voltage. This voltage loss can be accounted for by the complex mechanism involved

from precipitation of metal hydroxides near the cathode and desorption of metal ions at the anode during the test.

4. For electro-hydro-mechanical coupled loading consolidation, voltage and current are additional parameters recorded throughout the test with DAQ whereas pH of soil sample was calculated at the top, mid and bottom of the sample on successful completion of the test. This additional effect of electric gradient response resulted in early dissipation of pore water through the sample which was confirmed from the moisture content value obtained before and after the test.

In summary, coupled electro-hydro-mechanical consolidation proved to be a promising technology to improve the consolidation characteristics of fine-grained soils.

---

#### REFERENCES

- [1] K. Lee, V. Choa, S. H. Lee, and S. H. Quek, "Constant rate of strain consolidation of Singapore marine clay," *Géotechnique*, Vol. 43, No. 3, pp. 471–488, 1993, DOI: 10.1680/geot.1993.43.3.471.
- [2] Abdurrahman Feturi S. Huweg, "Modelling of Electrokinetic Phenomena in Soils," University of Southern Queensland Faculty, 2013.
- [3] J. Yuan, "Large strain analysis of electro-osmosis consolidation for clays," Hohai University, Nanjing, China, 2015.
- [4] V. Jeyakanthan, C. T. Gnanendran, and S. R. Lo, "Laboratory assessment of electro-osmotic stabilization of soft clay," *Can. Geotech. J.*, Vol. 48, No. August, pp. 1788–1802, 2011, DOI: 10.1139/T11-073.
- [5] C. H. Weng, Y. T. Lin, C. Yuan, and Y. H. Lin, "Dewatering of bio-sludge from industrial wastewater plant using an electrokinetic-assisted process: Effects of electrical gradient," *Sep. Purif. Technol.*, Vol. 117, pp. 35–40, 2013, DOI: 10.1016/j.seppur.2013.06.013.
- [6] M. Citeau, M. Loginov, and E. Vorobiev, "Improvement of sludge electro-dewatering by anode flushing," *Dry. Technol.*, Vol. 34, No. 3, pp. 307–317, 2016, DOI: 10.1080/07373937.2015.1052083.
- [7] M. Malekzadeh, "Electrokinetic dewatering and consolidation of dredged marine sediments." James Cook University, 2016.
- [8] M. K. Kherad, A. H. Vakili, M. R. bin Selamat, M. Salimi, M. S. Farhadi, and M. Dezh, "An experimental evaluation of electroosmosis treatment effect on the mechanical and chemical behavior of expansive soils," *Arab. J. Geosci.*, Vol. 13, No. 6, 2020, DOI: 10.1007/s12517-020-5266-3.
- [9] Z. J. Xue, C. G. Yan, and W. G. Li, "Coupling of electrochemical-temperature-mechanical processes in marine clay during electro-osmotic consolidation," *Sci.*

- Rep.*, Vol. 10, No. 1, pp. 1–13, 2020, DOI: 10.1038/s41598-020-70700-z.
- [10] S. Babu, R. Thirumalai, V. N. Nayak, and S. Gobinath, “Experimental investigation on expansive soils using electro kinetic geosynthetics (EKG) under cyclic loading,” *Mater. Today Proc.*, Vol. 37, pp. 1146–1153, 2021, DOI: 10.1016/j.matpr.2020.06.349.
- [11] L. Deleon, F. Romero, C. Gomes, and A. Carolina, “Electrokinetic dewatering of mine tailing: influence of solid content and voltage level applied,” 2022.
- [12] C. J. F. P. Jones, J. Lamont-Black, S. Glendinning, C. White, and D. Alder, “The environmental sustainability of electrokinetic geosynthetic strengthened slopes,” *Proc. Inst. Civ. Eng. Eng. Sustain.*, Vol. 167, No. 3, pp. 95–107, 2014, DOI: 10.1680/ensu.13.00015.
- [13] Z. Xue, X. Tang, Q. Yang, Z. Tian, Y. Zhang, and W. Xu, “Mechanism of electro-osmotic chemical for clay improvement: Process analysis and clay property evolution,” *Appl. Clay Sci.*, Vol. 166, No. September, pp. 18–26, 2018, DOI: 10.1016/j.clay.2018.09.001.
- [14] H. Zhou, Y. Fang, M. Chen, and W. Li, “Experimental analysis of the effect of mineral composition and water content of clay soil on electroosmotic efficiency,” *Bull. Eng. Geol. Environ.*, Vol. 80, No. 1, pp. 705–715, 2021, DOI: 10.1007/s10064-020-01945-1.
- [15] A. Deng and Y. Zhou, “Modeling electroosmosis and surcharge preloading consolidation. I: Model formulation,” *J. Geotech. Geoenvironmental Eng.*, Vol. 142, No. 4, pp. 1–8, 2016, DOI: 10.1061/(ASCE)GT.1943-5606.0001417.
- [16] L. Zhang, L. Jing, N. Wang, C. Fang, Y. Li, and Z. Shan, “Electro-Osmosis Chemical Treatment of High-Salinity Soft Marine Soils: Laboratory Tests,” *Open Civ. Eng. J.*, Vol. 11, No. 1, pp. 109–120, 2017, DOI: 10.2174/1874149501711010109.
- [17] F. Liu *et al.*, “Vacuum Preloading Combined with Intermittent Electro-Osmosis for Dredged Slurry Strengthening,” *Geotech. Test. J.*, Vol. 43, No. 3, pp. 775–790, 2020, DOI: 10.1520/GTJ20180234.
- [18] D. ASTM, “Standard test methods for one-dimensional consolidation properties of soils using incremental loading,” *D2435/D2435M-11*. 2011.
- [19] ASTM D854, “Standard Test Methods for Specific Gravity of Soil Solids by Water Pycnometer 1 ter ( Moisture ) Content of Soil and Rock by Mass Purposes ( Unified Soil Classification System ) Engaged in the Testing and / or Inspection of Soil and Rock Construction Mate,” *Annu. B. ASTM Stand.*, Vol. i, pp. 1–7, 2008.
- [20] D. ASTM, “Standard practice for classification of soils for engineering purposes,” *D2487*, 2007.
- [21] A. C. D.-18 on S. and Rock, “Standard Test Methods for Laboratory Determination of Water (moisture) Content of Soil and Rock by Mass,” 2005.
- [22] ASTM D4318, ASTM D 4318-10, and A. D4318-05, “Standard Test Methods for Liquid Limit, Plastic Limit, and Plasticity Index of Soils,” *Report*, Vol. 04, No. March 2010, pp. 1–14, 2005, DOI: 10.1520/D4318-10.
- [23] “astm d 698.pdf.”
- [24] D. ASTM, “Standard test method for pH of soils,” *D4972-01*, Vol. 4, 2001.
- [25] D. ASTM, “Standard Test Methods for Determining the Water (Moisture) Content, Ash Content, and Organic Material of Peat and Other Organic Soils,” *2974 - 20e1*, 1993.
- [26] J. Zhou, Y. L. Tao, C. J. Xu, X. N. Gong, and P. C. Hu, “Electro-osmotic strengthening of silts based on selected electrode materials,” *Soils Found.*, Vol. 55, No. 5, pp. 1171–1180, 2015.
- [27] S. Bourghès-Gastaud, P. Dolez, E. Blond, and N. Touze-Foltz, “Dewatering of oil sands tailings with an electrokinetic geocomposite,” *Miner. Eng.*, Vol. 100, pp. 177–186, 2017, DOI: 10.1016/j.mineng.2016.11.002.
- [28] D. J. Singh, B. R. Paramkusam, and A. Prasad, “Determination of Consolidation Parameters of Geomaterials Using Modified CRS Consolidation Testing System,” *KSCE J. Civ. Eng.*, pp. 1–14, 2021.
- [29] V. Jeyakanthan, C. T. Gnanendran, and S. R. Lo, “Laboratory assessment of electro-osmotic stabilization of soft clay,” *Can. Geotech. J.*, Vol. 1802, No. August, pp. 1788–1802, 2011, DOI: 10.1139/T11-073.
- [30] Z. J. Xue, C. G. Yan, and W. G. Li, “Coupling of electrochemical–temperature–mechanical processes in marine clay during electro-osmotic consolidation,” *Sci. Rep.*, Vol. 10, No. 1, pp. 1–14, 2020, DOI: 10.1038/s41598-020-70700-z.
- [31] A. N. Alshawabkeh, T. C. Sheahan, and X. Wu, “Coupling of electrochemical and mechanical processes in soils under DC fields,” *Mech. Mater.*, Vol. 36, No. 5–6, pp. 453–465, 2004.
- [32] V. Jeyakanthan, “ELECTRO-OSMOTIC STABILISATION OF SOFT SOILS SOILS – A NUMERICAL APPROACH,” 2009.
- [33] B. G. Ryu, J. S. Yang, D. H. Kim, and K. Baek, “Pulsed electrokinetic removal of Cd and Zn from fine-grained soil,” *J. Appl. Electrochem.*, Vol. 40, No. 6, pp. 1039–1047, 2010, DOI: 10.1007/s10800-009-0046-5.
- [34] R. López-Vizcaino *et al.*, “Scale-up on electrokinetic remediation: Engineering and technological parameters,” *J. Hazard. Mater.*, Vol. 315, pp. 135–143, 2016, DOI: 10.1016/j.jhazmat.2016.05.012.
- [35] H. Fu, L. Yuan, J. Wang, Y. Cai, X. Hu, and X. Geng, “Influence of High Voltage Gradients on Electrokinetic Dewatering for Wenzhou Clay Slurry Improvement,” *Soil Mech. Found. Eng.*, Vol. 55, No. 6, pp. 400–407, 2019, DOI: 10.1007/s11204-019-09555-0.
- [36] S. Yang, F. Jianting, S. Wen, and Q. Chenchen, “Effects of Voltage Gradients on Electro-Osmotic Characteristics of Taizhou Soft Clay,” Vol. 14, pp. 2136–2159, 2019, DOI: 10.20964/2019.03.06.
- [37] K. Y. Lo, K. S. Ho, and I. I. Incullet, “Field test of electroosmotic strengthening of soft sensitive clay,” *Can. Geotech. J.*, Vol. 28, No. 1, pp. 74–83, 1991.
- [38] J. Ukleja, “Stabilization of landslides sliding layer using electrokinetic phenomena and vacuum treatment,” *Geosci.*,

- Vol. 10, No. 8, pp. 1–23, 2020, DOI: 10.3390/geosciences10080284.
- [39] S. Y. J. Huey, “Consolidation of Peat and Organic Soil using Electro-osmosis Treatment,” Faculty of Engineering & Science Department, 2016.
- [40] H. Wu, L. Hu, and Q. Wen, “Electro-osmotic enhancement of bentonite with reactive and inert electrodes,” *Appl. Clay Sci.*, Vol. 111, pp. 76–82, 2015, DOI: 10.1016/j.clay.2015.04.006.
- [41] S. Gargano, S. Lirer, and A. Flora, “Analysis of the coupled electro-osmotic and mechanical consolidation in clayey soils,” *Proc. Inst. Civ. Eng. Gr. Improv.*, Vol. 172, No. 3, pp. 146–157, 2019, DOI: 10.1680/jgrim.18.00010.
- [42] N. J. Kollannur and D. N. Arnepalli, “Electrochemical treatment and associated chemical modifications of clayey soils: a review,” *Int. J. Geotech. Eng.*, Vol. 00, No. 00, pp. 1–10, 2019, DOI: 10.1080/19386362.2019.1653513.
- [43] V. A. Korolev and D. S. Nesterov, “Influence of electro-osmosis on physicochemical parameters and microstructure of clay soils,” *J. Environ. Sci. Heal. - Part A Toxic/Hazardous Subst. Environ. Eng.*, Vol. 54, No. 6, pp. 560–571, 2019, DOI: 10.1080/10934529.2019.1571321.
- [44] L. Zhang, L. Hu, L. Zhang, and H. Wu, “Experimental study of the effects of soil pH and ionic species on the electro-osmotic consolidation of kaolin Experimental study of the effects of soil pH and ionic species on the electro-osmotic consolidation of kaolin,” *J. Hazard. Mater.*, No. September, pp. 0–1, 2018, DOI: 10.1016/j.jhazmat.2018.09.015.
- [45] M. Malekzadeh and N. Sivakugan, “One-dimensional electrokinetic stabilization of dredged mud,” *Mar. Georesources Geotechnol.*, Vol. 35, No. 5, pp. 603–609, 2017, DOI: 10.1080/1064119X.2016.1213778.
- [46] A. Sachan, G. Vikash, and A. Prashant, “Development of Intermediate Microfabric in Kaolin Clay and Its Consolidation Behaviour,” *Geotech. Geol. Eng. An Int. J.*, 2012, DOI: 10.1007/s10706-012-9557-7.
- [47] H. Moayedi, R. Nazir, S. Kazemian, and B. K. Huat, “Microstructure analysis of electrokinetically stabilized peat,” *Meas. J. Int. Meas. Confed.*, Vol. 48, No. 1, pp. 187–194, 2014, DOI: 10.1016/j.measurement.2013.11.006.
- [48] S. Gargano, S. Lirer, B. Liguori, and A. Flora, “Effect of the pore fluid salinities on the behaviour of an electrokinetic treated soft clayey soil,” *Soils Found.*, Vol. 60, No. 4, pp. 898–910, 2020, DOI: 10.1016/j.sandf.2020.06.003.
- [49] S. R. Kaniraj, “Soft Soil Improvement by Electroosmotic Consolidation,” *Int. J. Integr. Eng.*, Vol. 6, No. 2, pp. 42–51, 2014.
- [50] S. Gargano, S. Lirer, B. Liguori, and A. Flora, “Effect of the pore fluid salinities on the behaviour of an electrokinetic treated soft clayey soil,” *Soils Found.*, Vol. 60, No. 4, pp. 898–910, 2020, DOI: 10.1016/j.sandf.2020.06.003.